Deficiency of Acetyltransferase *nat10* in Zebrafish Causes Developmental Defects in the Visual Function

Hou-Zhi Yang,[4] Donghai Zhuo,[1] Zongyu Huang,[4] Gan Luo,[4,5] Shuang Liang,[2] Yonggang Fan,[1] Ying Zhao,[1] Xinxin Lv,[1] Caizhen Qiu,[1] Lingzhu Zhang,[1] Yang Liu,[5] Tianwei Sun,[4,5] Xu Chen,[2,3] Shan-Shan Li,[1] and Xin Jin[1–3]

[1]School of Medicine, Nankai University, Tianjin, China
[2]Tianjin Central Hospital of Gynecology and Obstetrics, Tianjin, China
[3]Tianjin Key Laboratory of Human Development and Reproductive Regulation, Tianjin, China
[4]Tianjin Medical University, Tianjin, China
[5]Department of Spinal Surgery, Tianjin Union Medical Center, Tianjin, China

Correspondence: Xin Jin, School of Medicine, Nankai University, No. 94 Weijin Road, Nankai District, Tianjin 300071, China; xin.jin@nankai.edu.cn.
Shan-Shan Li, School of Medicine, Nankai University, No. 94 Weijin Road, Nankai District, Tianjin 300071, China; shanshan.li@nankai.edu.cn.
Xu Chen, Tianjin Central Hospital of Gynecology Obstetrics, Tianjin 300100, China; chenxu2665@126.com.

HZY, DZ and ZH contributed equally to this study.

Received: July 25, 2023
Accepted: January 19, 2024
Published: February 21, 2024

Citation: Yang HZ, Zhuo D, Huang Z, et al. Deficiency of acetyltransferase *nat10* in Zebrafish causes developmental defects in the visual function. *Invest Ophthalmol Vis Sci*. 2024;65(2):31. https://doi.org/10.1167/iovs.65.2.31

Purpose. N4-acetylcytidine (ac4C) is a post-transcriptional RNA modification catalyzed by N-acetyltransferase 10 (NAT10), a critical factor known to influence mRNA stability. However, the role of ac4C in visual development remains unexplored.

Methods. Analysis of public datasets and immunohistochemical staining were conducted to assess the expression pattern of *nat10* in zebrafish. We used CRISPR/Cas9 and RNAi technologies to knockout (KO) and knockdown (KD) *nat10*, the zebrafish ortholog of human NAT10, and evaluated its effects on early development. To assess the impact of *nat10* knockdown on visual function, we performed comprehensive histological evaluations and behavioral analyses. Transcriptome profiling and real-time (RT)-PCR were utilized to detect alterations in gene expression resulting from the *nat10* knockdown. Dot-blot and RNA immunoprecipitation (RIP)-PCR analyses were conducted to verify changes in ac4C levels in both total RNA and opsin mRNA specifically. Additionally, we used the actinomycin D assay to examine the stability of opsin mRNA following the *nat10* KD.

Results. Our study found that the zebrafish NAT10 protein shares similar structural properties with its human counterpart. We observed that the *nat10* gene was prominently expressed in the visual system during early zebrafish development. A deficiency of *nat10* in zebrafish embryos resulted in increased mortality and developmental abnormalities. Behavioral and histological assessments indicated significant vision impairment in *nat10* KD zebrafish. Transcriptomic analysis and RT-PCR identified substantial downregulation of retinal transcripts related to phototransduction, light response, photoreceptors, and visual perception in the *nat10* KD group. Dot-blot and RIP-PCR analyses confirmed a pronounced reduction in ac4C levels in both total RNA and specifically in opsin messenger RNA (mRNA). Additionally, by evaluating mRNA decay in zebrafish treated with actinomycin D, we observed a significant decrease in the stability of opsin mRNA in the *nat10* KD group.

Conclusions. The ac4C-mediated mRNA modification plays an essential role in maintaining visual development and retinal function. The loss of NAT10-mediated ac4C modification results in significant disruptions to these processes, underlining the importance of this RNA modification in ocular development.

Keywords: N-acetyltransferase 10 (NAT10), development, visual function, opsin, N4-acetylcytidine (ac4C), behavior, zebrafish

The formation of the visual system represents a highly complex biological process,[1] influenced by a complex interplay of genetic, epigenetic, and environmental factors.[2,3] From the earliest stages of embryonic development through to the fine-tuning of visual functions in childhood, various epigenetic modifications, such as DNA methylationm,[2] histone alterations,[4] and the activities of non-coding RNAs,[5] are essential. These modifications play critical roles in the differentiation of visual cells, the formation of neural networks in the visual system, and the visual system's adaptive response to environmental changes. However, the role of post-transcriptional modification of RNA in visual development is yet to be fully understood.

The advancements in sequencing technologies have led to the identification of over 100 distinct chemical modifications across a variety of RNA types.[6–10] Among these, N4-acetylcytidine (ac4C) has attracted increasing attention during in recent years. This is primarily because ac4C

represents the sole acetylation modification identified so far in eukaryotic messenger RNAs (mRNAs).[7,11] Recent evidence has illuminated the extensive impact of ac4C modifications in RNAs, underscoring their crucial role in RNA regulation across various biological levels.[12–14] In transfer RNAs (tRNAs), ac4C modifications are recognized for enhancing protein translation fidelity and have been linked to increased thermotolerance in organisms.[15,16] In ribosomal RNAs (rRNAs), ac4C modifications are distinctive features of thermophilic organisms, playing a critical role in facilitating precise protein translation.[17–19] The ac4C is also a notable modification found on mRNAs with significant impacts on their stability and translation efficiency. Studies identified ac4C primarily within the coding sequences of human mRNAs, demonstrating its association with increased mRNA stability.[20–22] The ac4C located at the wobble site was shown to enhance protein translation, suggesting a mechanism where ac4C stabilizes base-paired guanosine interactions during translation, thereby promoting efficiency.[22] Furthermore, Tardu et al. observed elevated levels of ac4C in yeast mRNAs under oxidative stress, suggesting a role for ac4C in stress response.[23] These findings highlight the crucial role of ac4C in maintaining the integrity and longevity of mRNA molecules, which ultimately ensures the sustained and efficient production of encoded proteins. Overall, ac4C exhibits multifaceted effects on post-transcriptional RNA modification, markedly improving mRNA stability and translation efficiency.

N-Acetyltransferase-like protein 10 (NAT10) has been identified as the first enzyme responsible for catalyzing the production of ac4C in eukaryotic RNA.[12–14,19] It possesses both acetyltransferase and RNA-binding activities, making it a key player in the ac4C modification process. The enzymatic process of ac4C formation, catalyzed by NAT10, requires acetyl-coenzyme A (CoA) as the acetyl group donor, and this reaction is supplied by the hydrolysis of either ATP or GTP.[18,24] Therefore, NAT10 plays a crucial role in the nucleolar modification of various RNA types, including the modification of yeast precursor rRNA at specific positions. In the context of tRNA, NAT10's activity is assisted by the THUMP domain-containing 1 (THUMPD1) protein,[15] whereas in rRNA, small nucleolar RNAs (snoRNAs) guide the ac4C modification process.[15] However, the specific cofactors involved in the NAT10-mediated formation of ac4C in mRNA have not yet been identified.

Recent studies have demonstrated the connection between ac4C modifications and the progression of various human diseases. It has been found that alterations in ac4C modifications, which are regulated by NAT10, can significantly impact the progression of diseases, such as bladder cancer.[25] This is primarily due to changes in the stability and translational efficiency of key genes. Liu et al. observed an increase in NAT10 expression in response to DNA damage, emphasizing the enzyme's crucial role in cell survival under stress conditions.[26] In addition, Balmus et al. reported that inhibiting NAT10 activity can reduce genomic instability and extend healthspan, while also alleviating age-related symptoms in a progeroid mouse model.[27] Furthermore, recent clinical research has identified a correlation between impaired tRNA acetylation and severe neurodevelopmental disorders in children. These disorders are characterized by a range of symptoms, including developmental delays, language impairments, intellectual challenges, and behavioral issues,[28] highlighting the importance of ac4c-mediated RNA modification in neurodevelopment. Further investigation has revealed that NAT10-catalyzed ac4C modification plays a critical role in maintaining pluripotency in human embryonic stem cells (hESCs).[21] It has shown a strong link between the expression of NAT10 and the state of pluripotency, indicating that both NAT10 and its enzymatic product, ac4C, are vital to the processes of self-renewal and differentiation in hESCs. However, the specific role of ac4C modification during visual development remains unknown.

In our study, we utilized a zebrafish animal model to investigate whether a reduction in ac4C modification, resulting from *nat10* deficiency, impacts visual development and behavior. By using CRISPR/Cas9 and RNA interference technologies, we successfully generated *nat10* knockout (KO) and knockdown (KD) zebrafish lines. Our results revealed that a deficiency of *nat10* in these zebrafish led to visual impairments. Through RNA sequencing analysis, we found that *nat10* KD predominantly disrupts retinal transcripts in zebrafish, a change that is associated with reduced levels of opsin mRNA ac4C content and stability. These findings highlight the critical role of NAT10-mediated ac4C modification in visual function during development.

Materials and Methods

Zebrafish Maintenance

All experimental procedures involving zebrafish were performed following the guidelines of the Institutional Animal Care and Use Committee (IACUC) and the Chinese Association for Laboratory Animal Science (CALAS). Our experimental protocols are designed to minimize potential distress to the animals and were approved by the Nankai University Animal Care and Use Committee.

Wild-type zebrafish (Danio rerio) of the A.B. strain were obtained from the National Zebrafish Resource Center. Adult zebrafish were housed in a dedicated aquaculture facility at a density of approximately five fish per liter, ensuring adequate space and environmental conditions conducive to their well-being. The facility maintained a 14-hour light/10-hour dark photoperiod to preserve the zebrafish's natural circadian rhythms. Water conditions were carefully regulated, with temperatures held between 27 and 29°C, a pH maintained at 7.0 ± 0.2, and an ion conductivity of 550 ± 10 µS/cm to replicate their natural aquatic habitat. Adult zebrafish received a balanced diet of brine shrimp twice daily, once in the morning and once in the evening. Fertilized eggs were collected and cultured in E3 medium under controlled conditions to ensure optimal development.

Generation of *nat10* Knockout and Knockdown Zebrafish

The CRISPR/Cas9 editing procedure in zebrafish has been previously described.[29] The guide RNA (gRNA) sequence targeting *nat10* was designed as 5′-CCACAGACCTGTGATCTTT-3′. The siRNA sequence was synthesized as 5′-CCACAGACCTGTGATCTTT-3′. For the generation of KOs, the injection cocktail was prepared with 100 pg of a gRNA lentiCRISPRv2GFP plasmid, which facilitates Cas9 and gRNA delivery. The KD mutants were created using the siRNA pLKO.1-EGFP-puro plasmid. A total of 200 zebrafish embryos underwent microinjection and subsequent screening to identify successful gene editing events.

Investigative Ophthalmology & Visual Science

Real-Time Quantitative Polymerase Chain Reaction

Total RNA was extracted from larval and adult zebrafish using the TRIzol reagent (Thermo Fisher Scientific, Waltham, MA, USA). According to the manufacturer's protocol, reverse transcription was performed using the TransScript One-Step gDNA Removal and cDNA Synthesis SuperMix kit (AT311; TransGen Biotech, Beijing, China). Then, Oligo dT primer (25 pmol) and Random Primer (50 pmol) were added to 20 µL of the mixture to obtain full-length cDNA efficiently. Next, RT-qPCR was performed using a QuantStudioTM 3 Real-Time PCR instrument (Thermo Fisher Scientific, USA) and PerfectStart Green qPCR SuperMix (AQ601; TransGen Biotech, Beijing, China), according to the manufacturer's instructions. Finally, we used the 2-ΔΔCT method to calculate the expression levels. The primers used for RT-PCR are listed below:

Gene	Forward Primer (From 5′-3′)	Reverse Primer (From 5′-3′)
opn1sw1	AGAAGTGTCCAGGATGGTTG TTGTG	AATACATGGCGGTGACGGCATAAG
opn1mw1	ATTCTTCGCAACACTTGGA GGTCAG	CATGTGAAAGCAATGCCAGCCATC
opn1mw2	GCTGTCATTTCTGCGTTCCTGTTAC	GACCATGCGTGTTACTTCCCTCTC
rho	AGCAGGAGTCCGAGACCACAC	CAGCAGATGAGGAAGGCGATGAC
opn1sw2	AAGATGGTGGTGGTAATGGT GTTCG	TTACAAAGGCAGGAGGGAAT GGTTG
opn1lw2	CAGCACAATCAGCGTCATCAATCAG	ACCACAGTCCAGCAATACCACATAC
nat10	GCTGCTGCTATTCCTCTGCCTTTAG	GCTCTGCTGTCGTAACTGCTGTATC

Behavioral Analysis

Open-field and Photomotor Response Tests: The open-field and photomotor responses were recorded using a DanioVision behavioral chamber (Noldus Information Technology, Wageningen, The Netherlands) at a rate of 25 frames per second. In the open-field behavioral assay, individual zebrafish larvae were placed in 6-well plates within the observation chamber. After a 30-minute acclimation period at 28°C, the freely moving zebrafish larvae were recorded for 10 minutes. Each arena was divided into center and border zones, and the time spent in each zone, as well as the total distance moved, were measured. In the photomotor response test, zebrafish larvae were individually placed in 24-well plates, with one larva per well. Following a 30-minute habituation period, the zebrafish larvae (6 dpf) were observed and recorded for an additional 30 minutes. The photomotor response was assessed through three light-dark transition cycles, each consisting of 5 minutes of light followed by 5 minutes of darkness. All behavioral tracking was performed using Noldus EthoVision XT video tracking software (version 13; Noldus Information Technology).

Light-dark preference (LDP) test: The LDP assay was conducted in plastic tanks (20 cm in length, 10 cm in width, and 20 cm in height). Each tank was divided into two equally sized compartments. To establish the dark conditions, half of each tank was covered with black tape, whereas the other half, designated as the light compartment, remained uncovered and was illuminated. After a 10-minute acclimation period, each zebrafish was transferred into the LDP assay. The zebrafish's movements were recorded for 10 minutes using a video camera fixed above the tank. The time spent in the dark and light compartments was analyzed using Noldus EthoVision XT video tracking software (version 13; Noldus Information Technology).

Novel Tank Diving (NTD) Test: The NTD test utilized a transparent, rectangular tank (25 cm in length, 5 cm in width, and 15 cm in height). This tank was divided into two equal horizontal sections by marking a centerline on the outer wall. The section above the centerline was designated as the "top" zone, whereas the section below was identified as the "bottom" zone. A video camera, strategically positioned to capture a lateral view, recorded the swimming behaviors of zebrafish placed individually in the tank for 10 minutes. The amount of time each zebrafish spent in the top zone and the frequency of their entries into the top zone were analyzed using Noldus EthoVision XT video tracking software.

Color Preference Test: The color preference test was conducted using a plus-shaped maze, consisting of four arms, each colored differently: red, yellow, blue, and green. The dimensions of each arm were 20 cm in length, 10 cm in width, and 10 cm in depth. At the center of the maze, a 10 cm cube functioned as the starting area for the zebrafish, referred to as the "blank" zone. The movement of zebrafish within the color preference setup was recorded from an overhead digital camera for a total duration of 30 minutes. The duration spent by zebrafish in various colored zones was quantitatively analyzed using Noldus EthoVision XT video tracking software. The color choice index for each pair color was calculated by determining the ratio of the time spent in each respective colored zone.

Optomotor Response Test (OMR): In OMR test, a single adult zebrafish was placed into a custom-designed circular tank. This tank contained a rotating drum, equipped with a pattern of black and white grating, rotating at a speed of 36 revolutions per minute (rpm). To set a contrast condition, half of the drum's inner surface was covered with white tape, thereby creating a distinct non-grating zone. The zebrafish's response to both stationary and rotating grating conditions was from an overhead digital camera for 5 minutes. Subsequently, the time spent by the zebrafish within the grating and non-grating zones was quantitatively assessed using the Noldus EthoVision XT video tracking software.

Transcriptome Sequencing and Bioinformatics Analysis

Total RNA from zebrafish samples was isolated utilizing TRIzol Reagent (Invitrogen Life Technologies, Waltham, MA, USA). The RNA's concentration, quality, and integrity were subsequently assessed with a NanoDrop spectrophotometer (Thermo Fisher Scientific, Waltham, MA, USA). We used three micrograms of RNA per sample for RNA library preparation, employing the TruSeq RNA Sample Preparation Kit (Illumina, San Diego, CA, USA). These libraries were sequenced on an Illumina HiSeq platform by Shanghai Personal Biotechnology Co., Ltd. Contaminating adaptor sequences were excised from the reads using Cutadapt software. Following the removal of low-quality and unidentified bases, the reads were aligned to the reference genome via HISAT2 software. Assembly of the mapped reads was conducted using StringTie software, and the transcriptomes from all samples were merged with gffcompare software to construct a comprehensive transcriptome. After the transcriptome assembly, StringTie and Ballgown were utilized for estimating the expression levels of all transcripts, calculating mRNA expression levels as FPKM. The identification of differentially expressed mRNAs was performed using the

Investigative Ophthalmology & Visual Science

R package DESeq2, with a selection criterion of log2 fold change ≥ 2 and P value < 0.01.

Gene Ontology enrichment analysis: The differentially expressed genes with their fold change values have been submitted to STRING Gene Ontology (GO) annotation enrichment analysis (https://string-db.org/).

Mapping the Temporospatial Expression Patterns of *nat10* During Zebrafish Development

To map the dynamic expression of *nat10*, we first assessed its regional gene expression across the early developmental stages of zebrafish using data from the ZFIN Gene Expression database (https://zfin.org/ZDB-GENE-040426-1543/expression).[30] We further investigated the *nat10* gene expression over time by analyzing an RNA-seq dataset from the EMBL-EBI Expression Atlas (http://www.ebi.ac.uk/gxa/experiments/E-ERAD-475).[31] For a detailed cellular-level perspective, we explored a single-cell RNA sequencing (scRNA-seq) dataset from the ZESTA database (https://db.cngb.org/stomics/datasets/STDS0000057).[32]

Assessment of Opsin mRNA Stability in Zebrafish

To determine the decay kinetics of opn1sw1 and opn1mw1 mRNAs, zebrafish from the negative control (NC) and the *nat10* KD groups were euthanized using 300 mg/L tricaine on ice. Subsequently, they underwent an intravitreal injection of 10 µL actinomycin D at a concentration of 100 µg/mL. Total RNA was extracted at five time points (0, 3, 6, 9, and 12 hours post-injection) and then reverse-transcribed. The levels of mRNA transcripts were quantitatively assessed using real-time quantitative PCR (RT-qPCR).

Histological Analysis

Following euthanasia using tricaine (300 mg/L) on ice, whole zebrafish were fixed in 4% paraformaldehyde. For a detailed anatomical study, eye sections were prepared by embedding the samples in paraffin and sectioning through the central region of the eye. These sections were stained with a 0.1% toluidine blue solution containing glacial acetic acid (G3668, Solarbio, China) for visualizing the retinal structure. Microscopic images of these sections were captured at 40 times magnification using a confocal microscope (Olympus FV1000).

For immunofluorescent staining, the sections were treated with an anti-HuC antibody (Cat# 55047-1-AP; Proteintech, China) and an anti-Nat10 antibody (Cat#: 13365–1-AP; Proteintech, China). The stained slides were then analyzed using ImageJ software (developed by Wayne Rasband, National Institutes of Health, Bethesda, MD, USA) to quantify and assess specific histological features.

Statistical Analysis

Statistical analyses were performed using GraphPad Prism version 7. The data are expressed as mean ± S.E. Differences between the two groups were analyzed using a two-tailed Student's *t*-test. For multiple-group comparisons, 1-way or 2-way ANOVA was conducted, followed by Tukey's multiple comparisons test. Differences were considered statistically significant at $P < 0.05$.

Results

Predominant *nat10* Expression in the Visual System During Early Development in Zebrafish

The zebrafish *nat10* gene contains 29 exons and 28 introns over a 28.06 kb genomic fragment on chromosome 18. It encodes a protein of 1025 amino acids containing multiple functional domains identical to the human homolog NAT10 protein (Fig. 1A). In addition, comparative analysis using AlphaFold's 3D protein structure predictions further reveals a core domain architecture in zebrafish NAT10 protein that is closely similar to its human homolog (Fig. 1B).

Using the ZFIN Gene Expression database (https://zfin.org/ZDB-GENE-040426-1543/expression), we found predominant *nat10* expression in eyes, optic tectum, and retina during early zebrafish development stages (Fig. 2A). Further analysis of a public RNA-seq dataset from the EMBL-EBI Expression Atlas (http://www.ebi.ac.uk/gxa/experiments/E-ERAD-475) revealed temporal variations in *nat10* expression (Fig. 2B), with peak activity during the gastrula segmentation stages. To understand the cellular-level spatial expression of *nat10* in zebrafish, we analyzed a scRNA-seq dataset from the ZESTA database (https://db.cngb.org/stomics/datasets/STDS0000057). The results revealed a dynamic and stage-specific expression pattern of *nat10* throughout zebrafish embryogenesis (Fig. 2C). Notably, *nat10* was prominently expressed in the optic vesicle region during early development, suggesting its potential significance in the developmental processes of the zebrafish visual system.

Nat10 Deficiency Leads to Developmental Abnormalities in Zebrafish Embryos

To investigate the effects of *nat10* deficiency on zebrafish embryonic development, KO and KD lines were generated using CRISPR/Cas9 and RNAi technologies (Fig. 3A). A reduction in *nat10* expression in these KO and KD lines was confirmed at both mRNA and protein levels (Figs. 3B, 3C). Histological analysis revealed a significant decrease in *nat10* expression across all retinal layers of the *nat10* KD zebrafish at various developmental stages, from 10 to 72 hours post-fertilization (hpf), compared to the NC group (Fig. 3D). Additionally, labeling of amacrine cells in the zebrafish retina with the HuC antibody indicated a notable reduction in their expression in the *nat10* knockdown group from 10 to 72 hpf (see Fig. 3D).

KO of *nat10* in zebrafish resulted in lethality, with embryos failing to survive beyond 72 hours post-fertilization (Fig. 4A). The survival rate in the *nat10* KD group was about 50% higher than that in the *nat10* KO group (see Fig. 4A). Additionally, both KO and KD of *nat10* in zebrafish significantly delayed embryo hatching when compared to the wild type (WT) and NC groups (Fig. 4B). The *nat10* KD group exhibited a survival rate approximately 50% higher than the *nat10* KO group (see Fig. 4A). Moreover, both KO and KD of *nat10* significantly delayed the hatching of zebrafish embryos compared to the WT and NC groups (see Fig. 4B). Morphological examinations during embryonic development revealed significant changes in the *nat10* KO and KD groups (Fig. 4C), including decreased body length (Fig. 4D) and severe tail bending in the larvae (Fig. 4E).

Investigative Ophthalmology & Visual Science

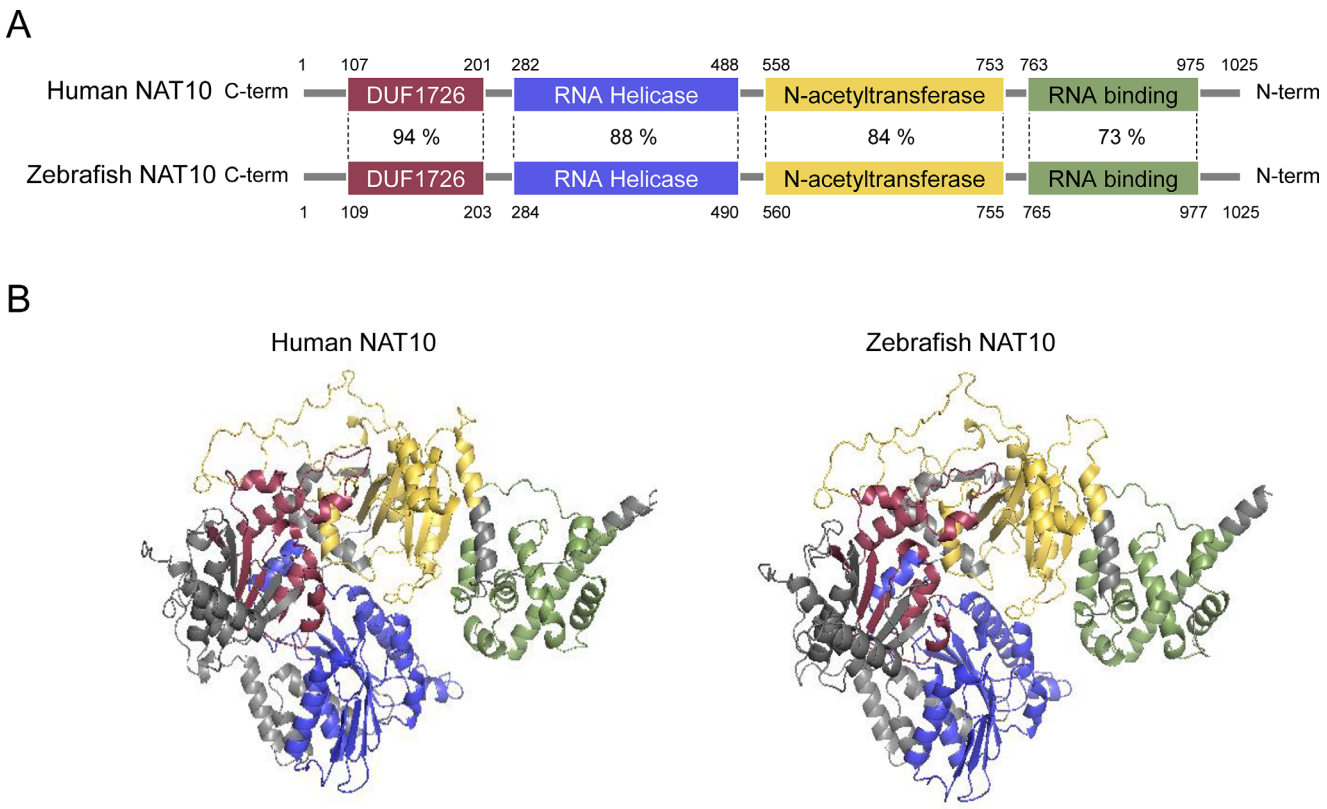

Figure 1. Comparative analysis of human and zebrafish NAT10 proteins. (**A**) Domain-wise percent sequence identity between human and zebrafish NAT10 proteins, highlighting their conserved regions. (**B**) Predicted three-dimensional (3D) structures of human and zebrafish NAT10 proteins using AlphaFold, with distinct domains, color-coded: DUF1726 (*purple*), RNA Helicase (*blue*), N-acetyltransferase (*yellow*), and RNA binding (*green*).

nat10 KD Increases Anxiety-Like Behavior in Zebrafish

We next explored the potential behavioral impacts of *nat10* deficiency during embryonic development in zebrafish larvae. Because *nat10* KO zebrafish do not survive beyond 72 hours postnatally, the *nat10* KD group was utilized to assess the behavioral effects of *nat10* deficiency. First, an open field test was conducted to evaluate locomotor activity differences between the NC and *nat10* KD larvae (Fig. 5A). We observed that *nat10* KD resulted in a significant decrease in both total travel distance and moving speed in 5-day post-fertilization (dpf) larvae compared to NC group (Fig. 5B). Furthermore, the *nat10* KD larvae exhibited a preference for the perimeter over the center of the field, frequently swimming along the walls rather than exploring the central area. This behavior is indicative of anxiety-like tendencies (see Fig. 5A). Consequently, the duration spent by larvae near the border was markedly increased in the *nat10* KD group compared to the NC group (Figs. 5C, 5D).

To further assess the potential anxiogenic effects of *nat10* KD in adult zebrafish, we conducted light-dark preference and novel tank assays. During the light-dark preference test, the swimming patterns of the *nat10* KD adult zebrafish revealed a marked preference for the dark area over the light zone (Fig. 5E). Compared to the NC group, the *nat10* KD group spent a significantly greater proportion of time in the dark zone (Figs. 5F, 5G). Similarly, in the novel tank assay, the *nat10* KD group exhibited a notable reduction in exploratory behavior (Fig. 5H), characterized by fewer entries into the tank's upper region (Fig. 5I) and extended durations in the bottom zone, as compared to the NC group (Fig. 5J). These results suggest that *nat10* deficiency leads to increased anxiety-like behaviors in zebrafish.

nat10 Deficiency Alters the Visual Perception and Color Recognition in Zebrafish

The *nat10* gene exhibits a pronounced expression in the eye, optic tectum, and retina during early developmental stages (see Fig. 1), implicating its potential role in visual system development. To evaluate the effects of *nat10* KD on visual perception, we conducted a visual-motor response assay (Fig. 6A). Following a 30-minute adaptation period, zebrafish were subjected to light-to-dark transitions every 5 minutes. Both the NC and *nat10* KD groups showed increased movement from light to dark and decreased movement from dark to light (see Fig. 6A). However, the *nat10* KD group displayed significantly less variability in movement during dark-to-light transitions compared to the NC group (Fig. 6B), suggesting a reduced visual response to light stimuli.

Further assessing visual motion deficits, the optomotor response of zebrafish to a rotating black/white grating was analyzed. In a transparent chamber with a rotating drum, the NC group exhibited robust optomotor responses to the grating (Fig. 6C). In contrast, the *nat10* KD group demon-

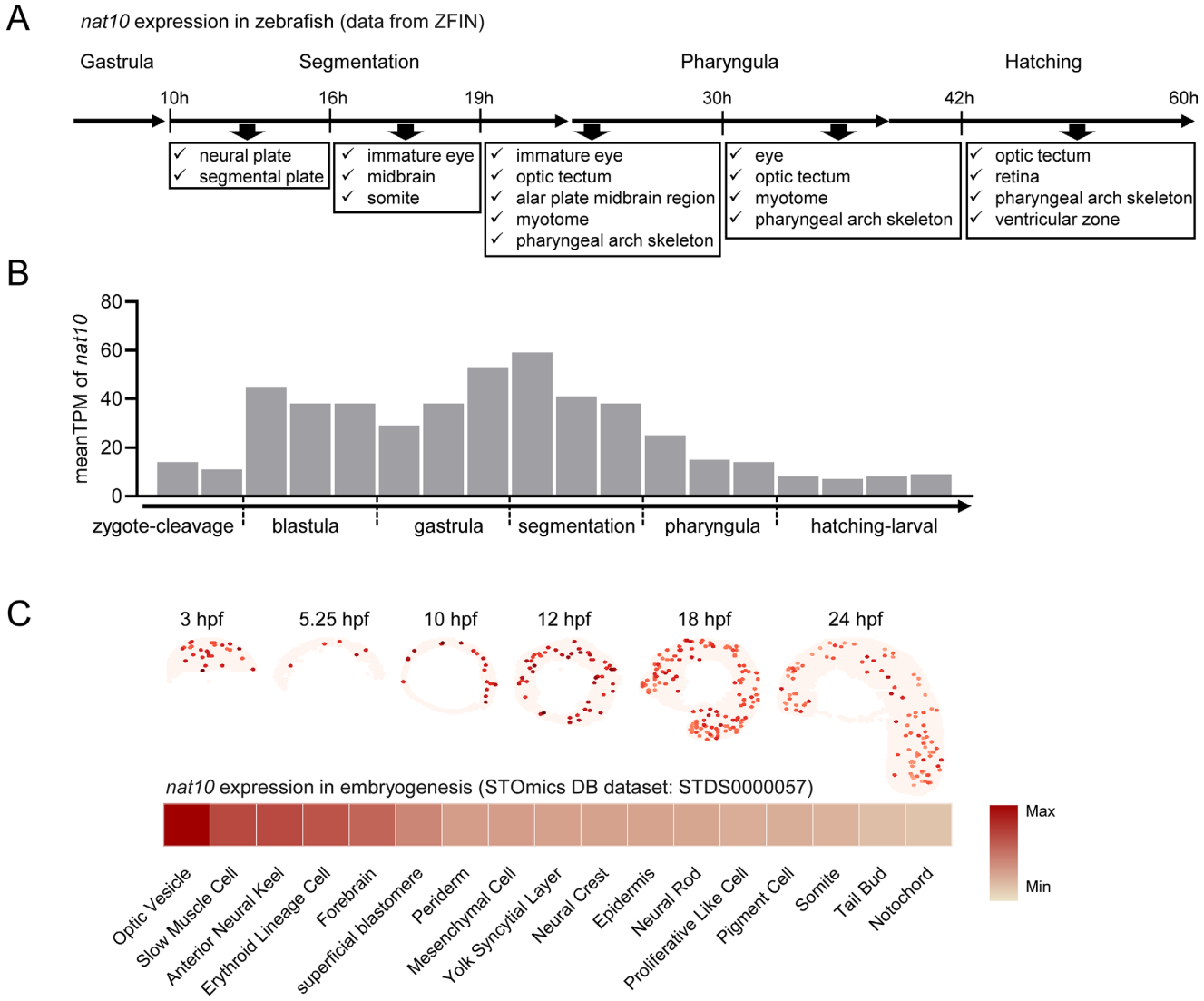

Figure 2. Spatiotemporal expression patterns of *nat10* in zebrafish. (**A**) A schematic representation delineating the spatial and temporal expression of *nat10* during zebrafish embryogenesis, as sourced from the Zebrafish Information Network (ZFIN, https://zfin.org/ZDB-GENE-040426-1543/expression). (**B**) A temporal expression profile of *nat10* mRNA throughout zebrafish embryonic development, derived from the Expression Atlas dataset (http://www.ebi.ac.uk/gxa/experiments/E-ERAD-475). (**C**) A comprehensive mapping of the spatiotemporal distribution of *nat10* expression in zebrafish embryogenesis using a dataset from the STOmics DB (https://db.cngb.org/stomics/datasets/STDS0000057). *Upper panel*: A detailed depiction of the spatial distribution of *nat10* expression across progressive developmental stages. *Lower panel*: A heatmap illustrating the mean expression levels of *nat10* in various spatial regions.

strated a lack of response and significantly less time spent in the grating zone (Fig. 6D). Additionally, we explored color preference using a cross maze with differently colored sleeves (Fig. 7A). The heatmap of swimming trails and color choice index revealed marked differences in the *nat10* KD group's movement in various color regions (Fig. 7B), indicating impaired color recognition.

We further investigated the morphological characteristics of *nat10* KD zebrafish. Retinal sections from the *nat10* KD group showed that the outer nuclear layer (ONL) and inner nuclear layer (INL) were thicker in the *nat10* KD group than in the NC group (Fig. 7C). Furthermore, the optic plexiform layer (OPL) in the *nat10* KD group was less dense, and disorganized, and its boundary with the INL blurred (see Fig. 7C). The observed alterations in retinal structure align with the behavioral findings, indicating that *nat10* KD contributes to compromised visual development in zebrafish. We further investigated the expression of HuC (ELAV-like neuron-specific RNA binding protein 3), known for its widespread presence in the nervous system and amacrine cells of the zebrafish retina during embryonic development. Immunofluorescence staining demonstrated a significant reduction in elavl3 expression in the *nat10* KD group compared to the NC group (Fig. 7D).

nat10 KD Predominantly Downregulates Retinal Transcripts

To investigate the molecular basis of visual function deficits in *nat10* KD zebrafish, we conducted genomewide transcriptome analysis using RNA-seq on 6 dpf larvae from both the NC and the *nat10* KD groups. RNA sequencing data revealed 1307 differentially expressed genes in the *nat10* KD group compared to the NC group, with log2 fold changes ≥2 and

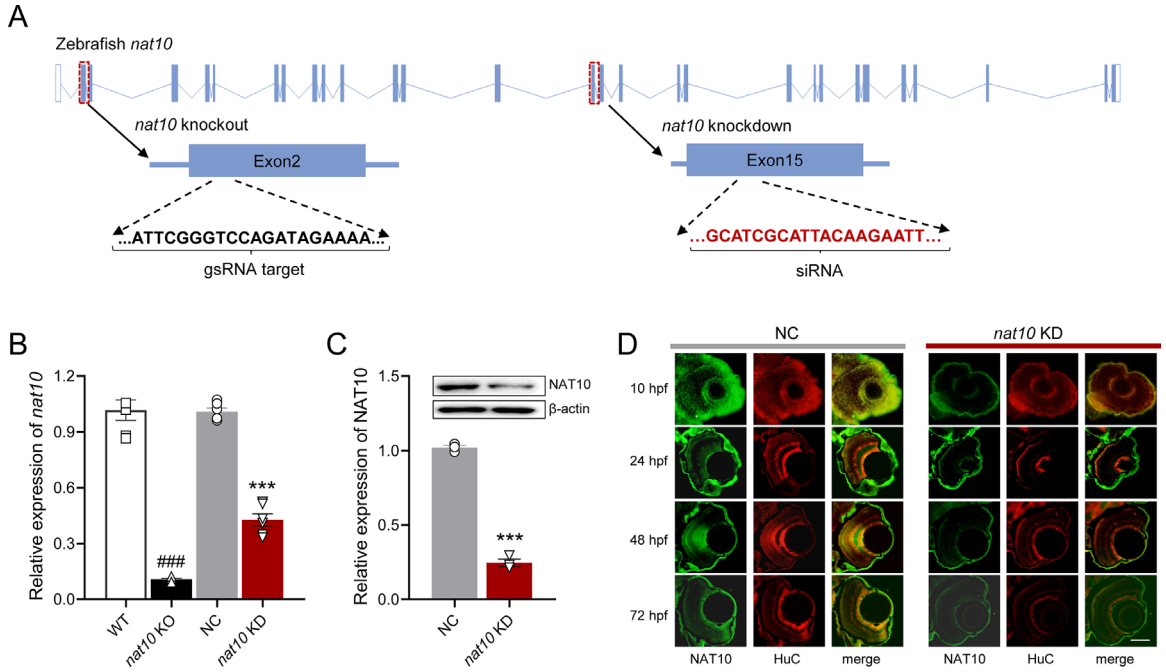

Figure 3. Disruption of *nat10* in zebrafish via CRISPR/Cas9 and siRNA. (**A**) Illustrates the genomic structure of the zebrafish *nat10* gene, highlighting the CRISPR/Cas9 target site in exon 2 (*orange underline*) and the siRNA target site in exon 15 (*red underline*) for knockout and knockdown, respectively. (**B**) Quantitative analysis of *nat10* mRNA expression levels in wild-type (WT), *nat10* knockout (KO), negative control (NC), and *nat10* knockdown (KD) zebrafish using real-time PCR. Results are presented as mean ± SEM from six independent experiments. Statistical analysis was performed using 1-way ANOVA with the Tukey post hoc test; ###$P < 0.001$ vs. WT, ***$P < 0.001$ vs. NC. (**C**) Western blot analysis of NAT10 protein expression in NC and *nat10* KD zebrafish. Data are expressed as mean ± SEM from 3 independent experiments, analyzed with an unpaired two-tailed Student's *t*-test; **$P < 0.01$ vs. NC. (**D**) Histological sections stained with NAT10 (*green*) and HuC (*red*) from NC and *nat10* KD zebrafish retinas at 10 hpf, 24 hpf, 48 hpf, and 72 hpf. Scale bar = 50 µm.

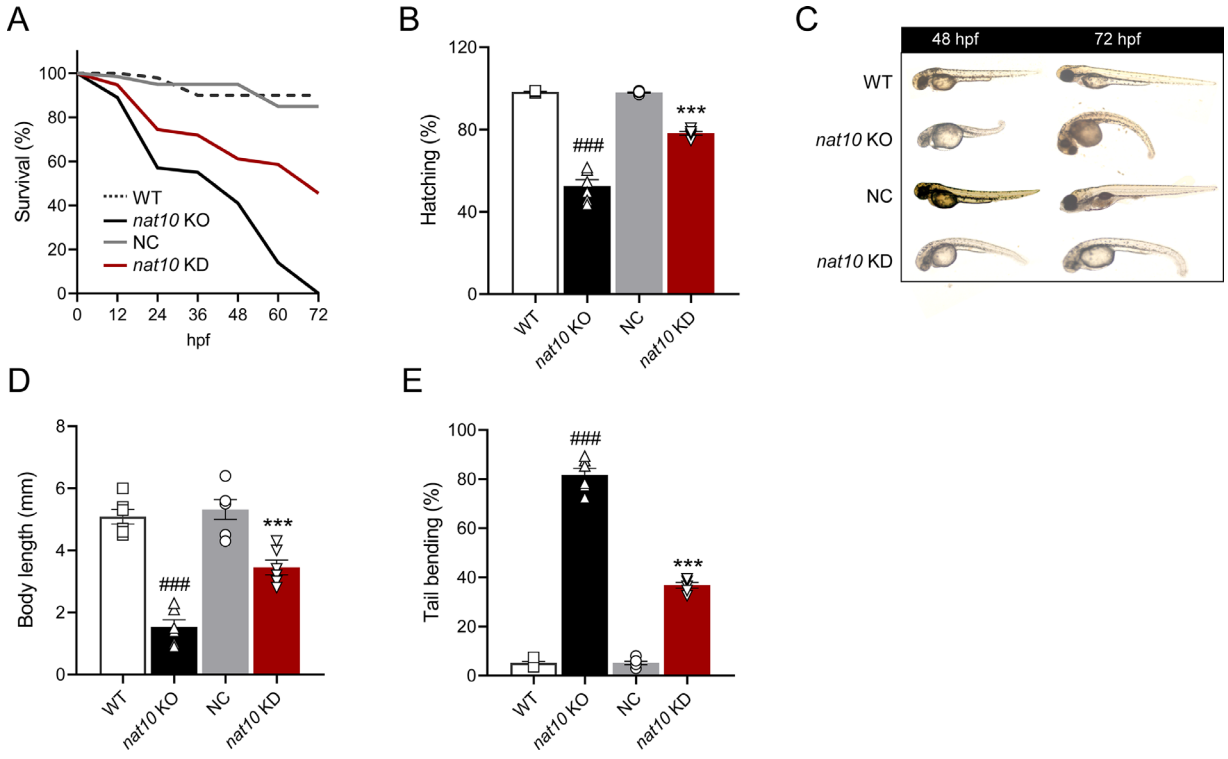

Figure 4. Impact of *nat10* deficiency on zebrafish embryonic development. (**A**) Displays the morphological phenotypes observed in WT, *nat10* KO, NC, and *nat10* KD zebrafish at 48 and 72 hours post-fertilization (hpf). Percent survival (**B**), percent hatching (**C**), body length (**D**), and percent tail bending (**E**) were compared among these groups. Results are presented as mean ± SEM from six independent experiments. Statistical analysis was performed using 1-way ANOVA with the Tukey post hoc test; ###$P < 0.001$ vs. WT, ***$P < 0.001$ vs. NC.

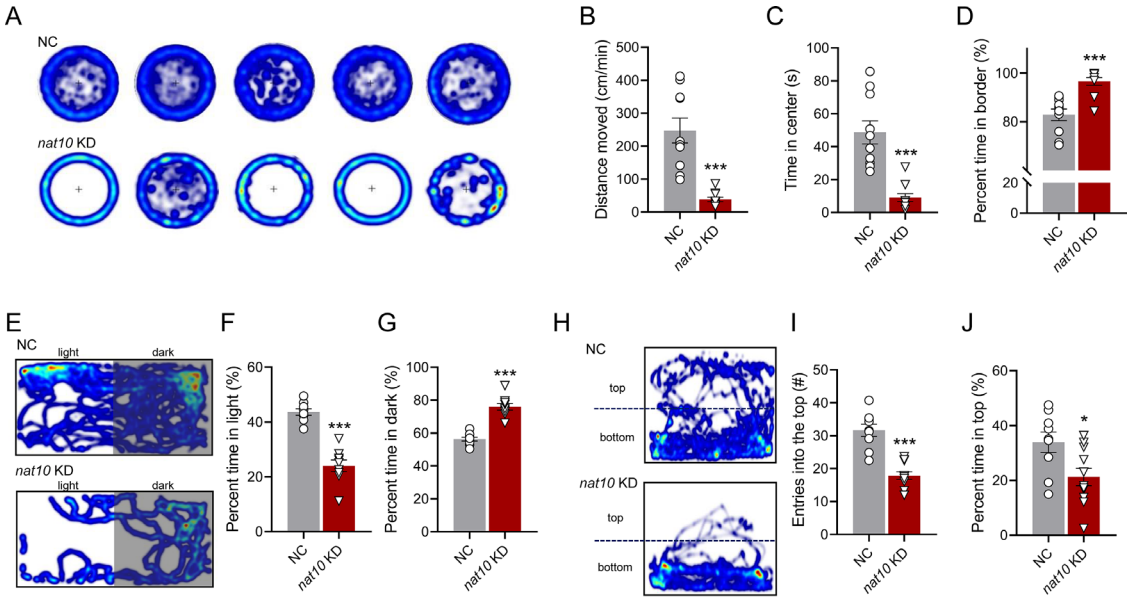

Figure 5. The *nat10* KD induces anxiety-like behaviors in zebrafish larvae. (**A**) A representative heat map traces the open field behavior over 10 minites, comparing NC and *nat10* KD zebrafish larvae; the *upper* and *lower panels* show NC and *nat10* KD larvae, respectively. Behavioral parameters assessed in the open field test include (**B**) total distance moved, (**C**) time spent in the center, and (**D**) percentage of time in the border area. (**E**) A representative heat map traces from the light-dark preference test over 10 minutes; *upper* and *lower panels* for NC and *nat10* KD larvae, respectively. Behavioral parameters assessed in the light-dark preference test are (**F**) percentage of time in the light zone and (**G**) in the dark zone. (**H**) A representative heat map traces from the novel tank diving test over 10 minutes, *upper* and *lower panels* for NC and *nat10* KD larvae, respectively. Analyzed behaviors in the novel tank diving test include (**I**) the number of entries into the top zone and (**J**) the percentage of time spent there. Results are presented as mean ± SEM from 9 to 11 independent experiments. Statistical analysis was performed using an unpaired two-tailed Student's *t*-test; $^{*}P < 0.0$, $^{***}P < 0.001$ vs. NC.

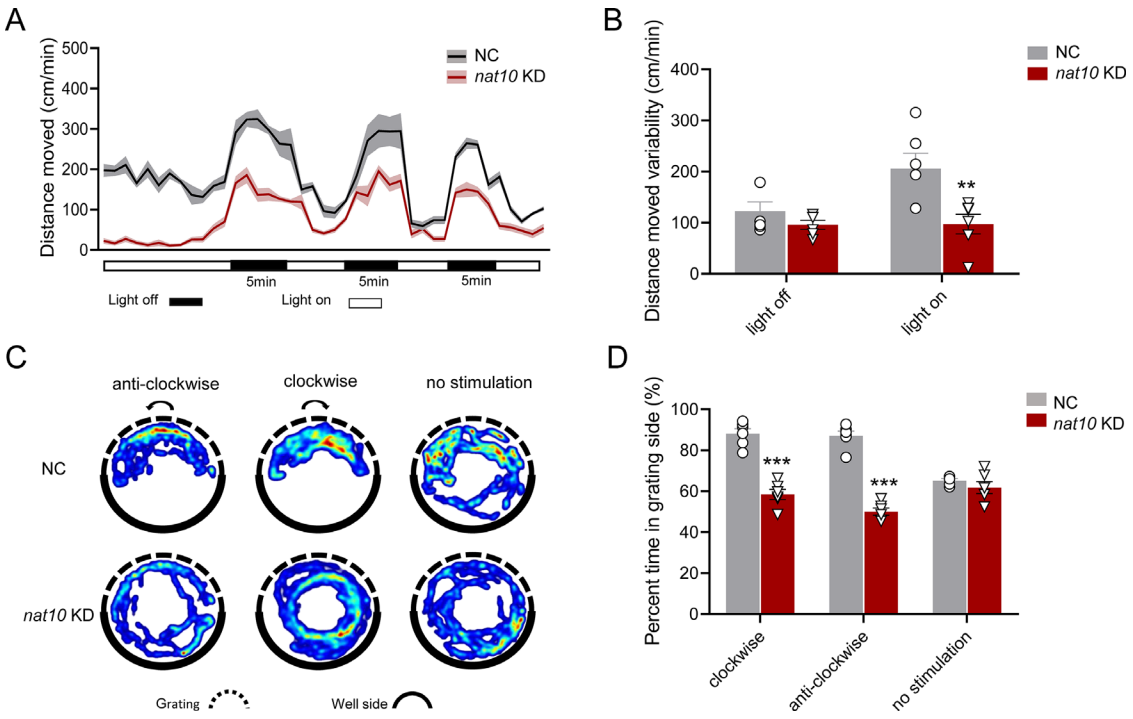

Figure 6. Effect of *nat10* KD on visual perception in zebrafish larvae. (**A**) Graph illustrating the locomotor response of zebrafish larvae to alternating light-dark conditions, with periods of 5 minutes each in darkness and light. The plot graph compares the average distances moved by larvae in the NC and the *nat10* KD groups, with the shaded areas representing the standard error of the mean (SEM). (**B**) Analyze the variability in movement during dark-light and light-dark transitions between the NC and the *nat10* KD groups. Results are presented as mean ± SEM from six independent experiments. Statistical analysis was performed using 2-way ANOVA with the Tukey post hoc test; $^{**}P <$ 0.001 vs. NC. (**C**) Representative heat map images showing the optomotor responses of zebrafish larvae to rotating grating over 5 minutes; *upper* and *lower panels* for the NC and the *nat10* KD zebrafish larvae, respectively. (**D**) The percentage of time zebrafish larvae spent on the grating side was in the NC and the *nat10* KD groups. Results are presented as mean ± SEM from six independent experiments. Statistical analysis was performed using 2-way ANOVA with the Tukey post hoc test; $^{***}P < 0.001$ vs. NC.

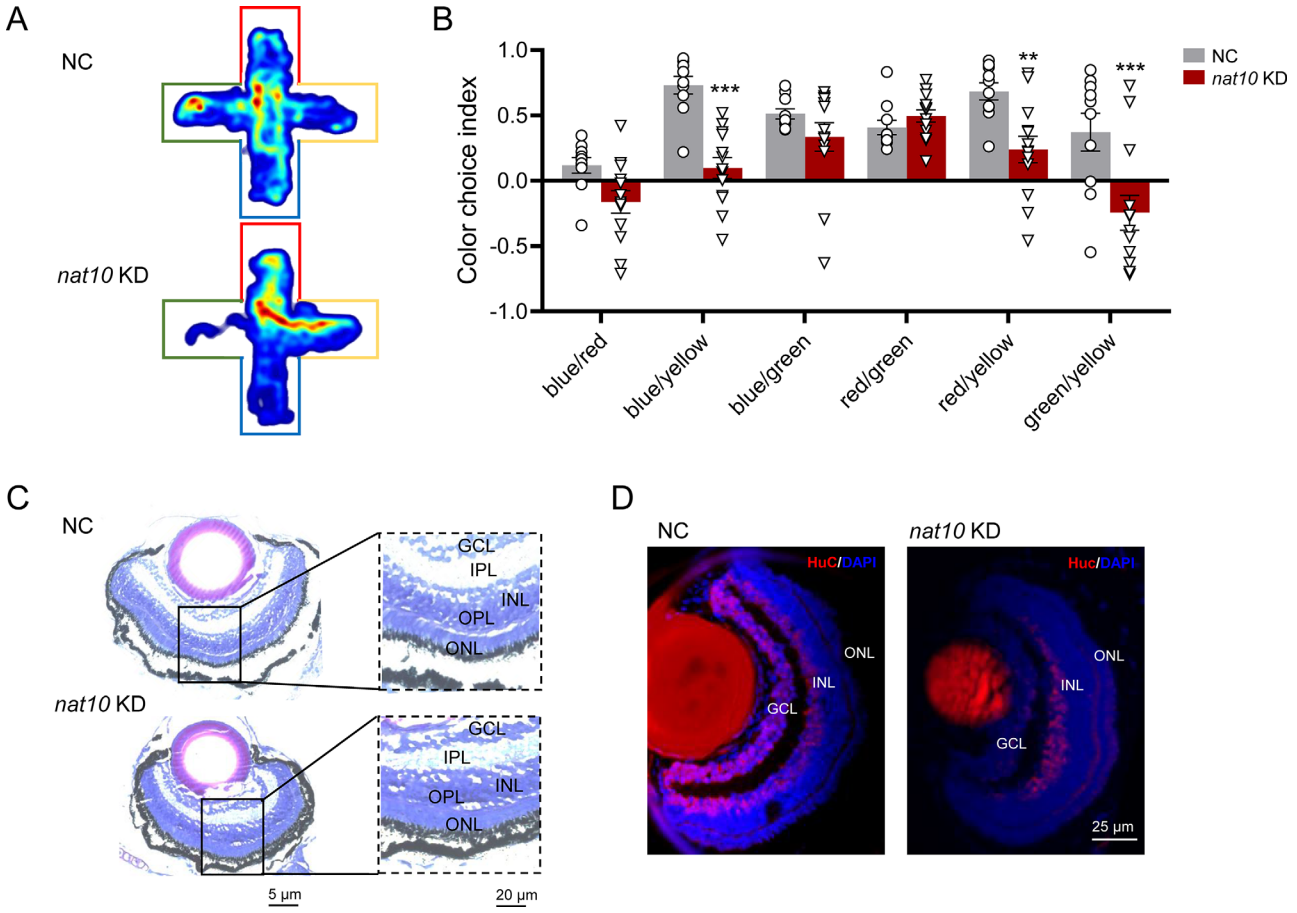

Figure 7. Influence of *nat10* KD on color preference and retinal morphology in zebrafish. (**A**) Representative heat map images showing the innate color preference behavior of zebrafish in a 10 minutes test within a plus-maze, each arm of which is covered with red, blue, yellow, and green sleeves; *upper* and *lower panels* for the NC and the *nat10* KD zebrafish larvae, respectively. (**B**) The calculation of the color choice index is based on the ratio of time spent in each two-color combination. Results are presented as mean ± SEM from 10 independent experiments. Statistical analysis was performed using 2-way ANOVA with the Tukey post hoc test; $^{**}P < 0.001$, $^{***}P < 0.001$ vs, NC. (**C**) Coronal sections of the retinas from the NC (*upper panel*) and the *nat10* KD (*lower panel*) zebrafish larvae; GCL, ganglion cell layer; INL and ONL, inner and outer nuclear layer, respectively; IPL and OPL, inner and outer plexiform layers. (**D**) Immunofluorescence staining of the retinas of the NC (*left panel*) and the *nat10* KD (*right panel*) zebrafish larvae with *elavl3* (*red*) and DAPI (*blue*).

P values ≤ 0.01, including 532 upregulated and 775 downregulated genes (Figs. 8A, 8B).

The GO analysis of these differentially regulated transcripts identified top-ranking clusters predominantly associated with phototransduction, photoreceptor outer segment, and G protein-coupled photoreceptor activity (Fig. 8C). Notably, gene transcripts crucial for phototransduction, such as opn1sw1, opn1mw1, prph2b, opn1mw2, rom1a, rho, opn1sw2, and opn1lw2, were significantly decreased in the *nat10* KO group (see Fig. 8C). Confirming the RNA-seq findings, RT-qPCR analysis showed downregulation of key opsin genes, including opn1sw1, opn1mw1, opn1mw2, rho, opn1sw2, and opn1lw2 (Fig. 8D). These findings demonstrate that *nat10* KD results in a substantial downregulation of genes essential for visual function.

nat10 KD Reduces ac4C Modification and Affects Opsin mRNA Stability

To assess the effects of *nat10* KD on the content of ac4C modifications in zebrafish larvae, we performed ac4C dot blotting and acetylated RNA immunoprecipitation (RIP-PCR) studies on RNA samples from the *nat10* KD and the NC groups. Initially, zebrafish larvae were transfected with *nat10* siRNA, and RNA was subsequently pulled down using an anti-ac4C antibody, with input and IgG serving as controls. The samples were analyzed via qRT-PCR. We found a significant reduction in the ac4C content of total RNA in the *nat10* KD group compared to the NC group (Fig. 9A). Furthermore, RIP-PCR results indicated a marked decrease in ac4C levels in mRNAs encoding opsin photoreceptors (opn1sw1, opn1sw2, opn1mw1, opn1mw2, and opn1lw2) in the *nat10* KD group (Figs. 9B, 9C).

Given Nat10's role in regulating gene expression via its influence on mRNA stability and translation efficiency, we examined RNA decay in zebrafish larvae following *nat10* KD. Larvae from both the NC and *nat10* KD groups were treated with actinomycin D to study the RNA stability over time. The decay curves demonstrate that the half-lives of opn1sw1 (Fig. 9D) and opn1mw1 (Fig. 9E) mRNAs are significantly reduced in the *nat10* KD group compared to the NC group, indicating compromised stability of opsin mRNA upon *nat10* KD. These results imply that *nat10* may affect visual function by modulating ac4C modification, which in

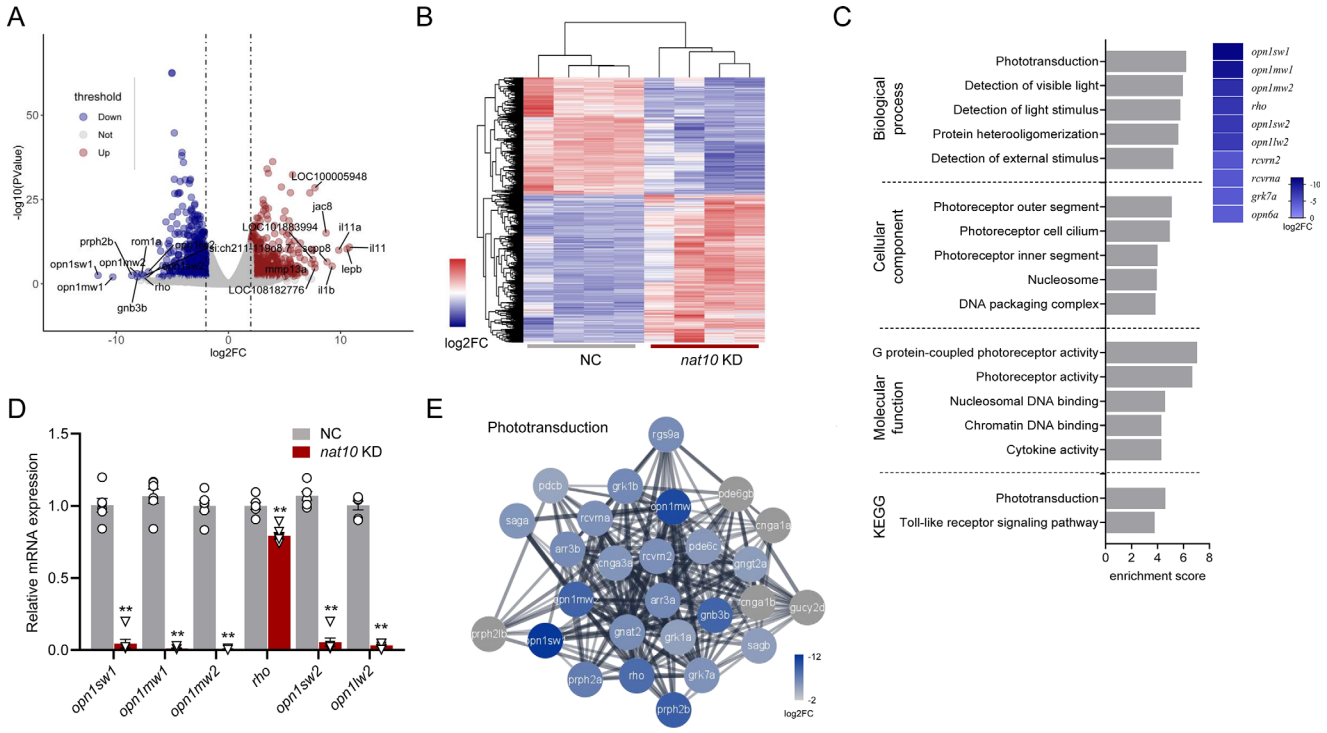

Figure 8. Transcriptomic profiling of *nat10* KD in zebrafish larvae. (**A**) Volcano plots illustrate the differential gene expression between the NC and the *nat10* KD zebrafish larvae. Differentially expressed genes, indicated by $P < 0.05$ and a log2 fold change (log2FC) ≥ 2 (downregulated genes in *blue*, upregulated genes in *red*, and nonsignificant changes in *gray*). (**B**) A hierarchical heatmap shows the differential expression patterns in 4 independent NC and *nat10* KD samples, with color intensity indicating fold changes; upregulation and downregulation are marked in *red* and *blue*, respectively. (**C**) Gene Ontology (GO) enrichment analysis for genes differentially expressed in *nat10* KD larvae, showing the top 5 GO terms in four categories ranked by enrichment score. The *right panel* shows a heatmap of genes associated with the phototransduction GO term, with a color scale reflecting log2FC. (**D**) Quantitative real-time RT-PCR validation of mRNA levels for key differentially expressed genes in phototransduction. Results are presented as mean ± SEM from six independent experiments. Statistical analysis was performed using 1-way ANOVA with the Tukey post hoc test; ***$P < 0.001$ vs. NC. (**E**) Construction of a protein-protein interaction network for the phototransduction interactome using STRING database.

turn impacts the stability of mRNAs related to retinal function in zebrafish.

Discussion

Recent discoveries highlighting the functions of chemical modifications RNA in various biological processes have suggested potential regulatory roles in neurodevelopment.[33,34] The ac4C is a post-transcriptional mRNA modification known to influence mRNA stability and translation efficiency.[11–13] However, its specific role in visual development remains underexplored. In our current study, we aimed to reduce ac4C modification in zebrafish by either knocking out or knocking down the expression of NAT10, the sole enzyme known for ac4C formation.[22] Our results revealed that a deficiency in NAT10-mediated ac4C modification led to developmental defects in the visual system and altered behavior.

A previous study in human HeLa cells indicated that deletion of the NAT10 gene reduces ac4C modification in mRNAs linked to cell survival and proliferation, thereby impacting their transcriptional efficiency and stability during translation.[22] In contrast, ac4C mRNA modification was found to enhance proliferation and metastasis in human tumor cell lines.[25] However, the influence of ac4C-related mRNA modification on the developmental process in animals has not been fully elucidated. The zebrafish ortholog of NAT10 protein shares significant amino acid similarity and protein domain structure with its human counterparts (see Fig. 1), suggesting potential conservation of NAT10's molecular function between humans and zebrafish. In our zebrafish model, *nat10* deficiency led to severe growth retardation, embryonic lethality, and structural malformations during early development, with survival not extending beyond 72 hours post-fertilization (hpf). In comparison, RNA interference (RNAi) injections in zebrafish embryos reduced *nat10* gene expression by approximately 50%, while simultaneously allowing a higher overall survival rate of up to 50%. This finding aligns with a previous study that showed that a complete loss of Nat10 results in embryonic lethality in mice, whereas heterozygous mice remain viable.[27] Consequently, our results, in conjunction with the findings of Balmus et al.,[27] underscore the critical importance of NAT10-mediated ac4C modification during early developmental stages.

Nat10 is prominently expressed in the retina during the early embryonic stages of zebrafish, indicating its potential role in the development of the visual system. The vertebrate retina, a highly organized and architecturally complex tissue within the CNS, plays a critical role in detecting and processing visual stimuli for the brain. Its development originates from an outgrowth of the diencephalon during embryonic stages and is meticulously regulated by genetic and epigenetic programs. Although the genetic aspects of retinal development have been extensively studied, the epige-

Investigative Ophthalmology & Visual Science

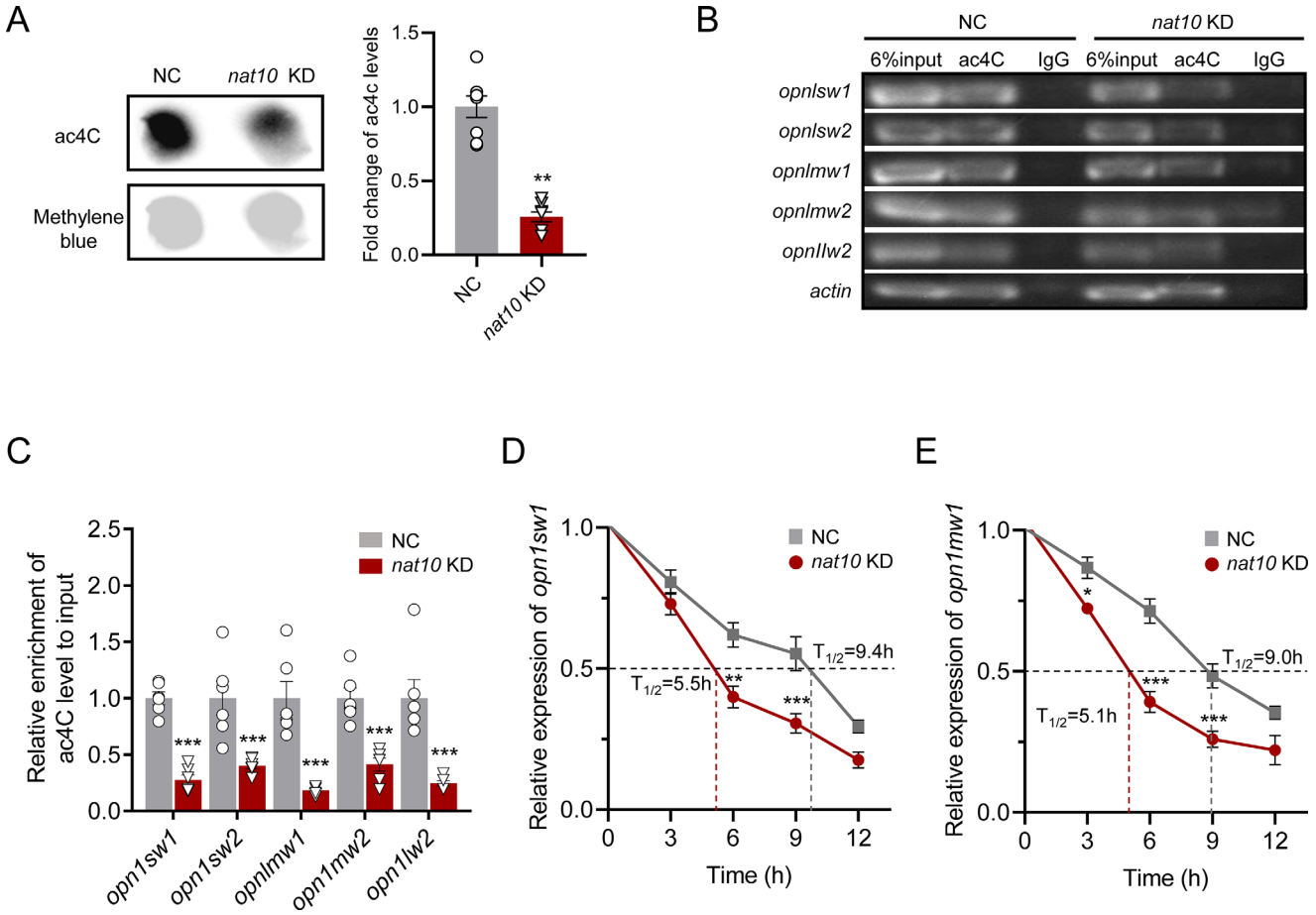

Figure 9. Impact of *nat10* KD on ac4C levels and mRNA stability in opsins. (**A**) *Right panel*: A representative dot blot displaying ac4C levels in total RNA from the NC and *nat10* KD zebrafish larvae. *Left panel*: Quantitative analysis of ac4C content in total RNA from both the NC and the *nat*10 KD groups, with results shown as mean ± SEM from eight independent experiments. Statistical analysis was performed using an unpaired two-tailed Student's *t*-test; ***$P < 0.001$ vs. NC. (**B, C**) RNA immunoprecipitation-PCR (RIP-PCR) analysis illustrating ac4C modifications in specific opsin mRNAs (opn1sw1, opn1sw2, opn1mw1, opn1mw2, opn1lw2, prph2b, and rom1a) in the NC and *nat10* KD larvae, presented as mean ± SEM from six independent experiments. Statistical analysis was performed using 2-way ANOVA with the Tukey post hoc test; ***$P < 0.001$ vs. NC. (**D, E**) The stability of opn1sw1 (**D**) and opn1mw1 (**E**) mRNAs at five time points (0-12 hours) after actinomycin-D treatment, was quantified via RT-PCR. Results are presented as mean ± SEM from six independent experiments, with mean terminal half-lives ($t_{1/2}$) indicated. Statistical analysis was performed using 2-way ANOVA with the Tukey post hoc test; *$P < 0.001$, ***$P <$ 0.001 vs. NC.

netic control mechanisms, particularly those involving ac4C-related mRNA modification, are not yet well understood. The *nat10* KD zebrafish in our study displayed a range of visual abnormalities, including defects in motion perception, altered color preferences, and a diminished response to light stimulation. Furthermore, our histological and immunohistochemical analyses indicated a disorganization of retinal layers and a reduction in the expression of the early neuron differentiation marker HuC in the retinas of *nat10* KD zebrafish. HuC, a well-known neuronal marker, is effective in labeling the presence and distribution of retinal neurons, particularly amacrine cells. The observed decrease in HuC expression suggests a potential loss of amacrine cells in *nat10* KD zebrafish. Amacrine cells play a critical role in the modulation of bipolar cell and retinal ganglion cell activities, influencing the adaptive properties essential for the functional diversity of retinal output. They are also integral in balancing color circuits within the retina. The impairment or loss of these cells in *nat10* KD zebrafish could significantly impact these crucial visual processing functions. However, the retina comprises a diverse array of cell types, each with a unique contribution to visual function. To fully elucidate the specific role of *nat10* in retinal development and function, further research is needed to investigate the impact of *nat10* deficiency on various retinal cell subpopulations, which will provide a more comprehensive understanding of its role in the maintenance of visual function.

In line with the observed visual abnormalities and distinct retinal morphological characteristics, our RNA sequencing analysis of *nat10* KD in zebrafish revealed notable downregulation of opsin genes critical for phototransduction. These genes include *opn1sw1*, *opn1mw1*, *opn1mw2*, *rho*, *opn1sw2*, and *opn1lw2*. Additionally, NAT10 is recognized as a key regulator of mRNA stability and translation via its role in ac4C formation. Our ac4C RIP-PCR analysis indicated a significant reduction in ac4C levels on RNA transcripts of these opsin photoreceptor genes in the *nat10* KD zebrafish. Furthermore, actinomycin D assays confirmed that the KD of *nat10* markedly reduces the mRNA stability of

opsin mRNA. Complementing our findings, various studies have highlighted NAT10's role in mRNA stability, particularly in the context of cancer. For instance, research has demonstrated that NAT10 is crucial for UVB-induced DNA damage repair by enhancing the mRNA stability of DDB2.[35] In colon cancer, NAT10 has been shown to affect the mRNA stability and expression of ferroptosis suppressor protein 1 (FSP1).[36,37] Additionally, NAT10's role in promoting the progression and metastasis of pancreatic ductal adenocarcinoma (PDAC) has been observed, where it stabilizes specific mRNAs in an ac4C-dependent manner.[38] Overall, our study provides important insights into the role of NAT10 in the visual system, particularly in promoting the stability of opsin mRNA in an ac4C-dependent manner. This mechanism could play a significant role in regulating retinal functions.

A limitation of our study is the absence of electroretinography (ERG) evaluation data. ERG is an important diagnostic tool for assessing retinal functionality,[39] particularly that of photoreceptors and inner retinal cells. Including ERG data would provide valuable insights into the functional status of photoreceptors, especially in light of the observed downregulation of opsin-related genes. Future research should incorporate comprehensive functional assessments like ERG to understand the impact of NAT10 modifications on visual function.

In conclusion, we generated knockout and knockdown conditions models of *nat10* in zebrafish to investigate the role of ac4C modification in visual development. Our findings demonstrated that NAT10-mediated ac4C modification plays a critical role in preserving normal visual function and behavior during zebrafish development. This study underscores the significance of ac4C modification in the developmental biology of visual systems.

Acknowledgments

The authors would like to thank the Busch-Nentwich laboratory for providing RNA-seq data. We thank the Zebrafish Information Network (ZFIN) and Spatial Transcript Omics DataBase (STOmics DB).

Data Availability: The data in support of the results are available from the corresponding author upon reasonable request.

Author Contributions: Acquisition of data: Hou-Zhi Yang, Donghai Zhuo, and Gan Luo. Data analysis: Hou-Zhi Yang, Donghai Zhuo, Gan Luo, Shuang Liang, Yonggang Fan, Ying Zhao, Xinxin Lv, Caizhen Qiu, Lingzhu Zhang, Yang Liu, Tianwei Sun, and Xu Chen. Writing of the manuscript: Hou-Zhi Yang, Shan-Shan Li, and Xin Jin. Review and/or revision of the manuscript: Hou-Zhi Yang, Shan-Shan Li, and Xin Jin. Conception and design: Shan-Shan Li and Xin Jin. Study supervision: Xin Jin.

Funded by the National Natural Science Foundation of China, grant number 81971083; National Natural Science Foundation of China, grant number 81770054; The Open Fund of Tianjin Central Hospital of Gynecology Obstetrics / Tianjin Key Laboratory of human development and reproductive regulation, grant number 2022XHY01; Tianjin Municipal Science and Technology Project, grant number 21JCZDJC00080. Tianjin Key Medical Discipline (Specialty) Construction Project, grant number TJYXZDXK-064B; Tianjin Health Research Project, grant number TJWJ2022MS018.

Disclosure: **H.-Z. Yang**, None; **D. Zhuo**, None; **Z. Huang**, None; **G. Luo**, None; **S. Liang**, None; **Y. Fan**, None; **Y. Zhao**, None; **X. Lv**, None; **C. Qiu**, None; **L. Zhang**, None; **Y. Liu**, None; **T. Sun**, None; **X. Chen**, None; **S.-S. Li**, None; **X. Jin**, None

References

1. Atkinson J, Braddick O. Visual development. *Handb Clin Neurol*. 2020;173:121–142.
2. Alkozi HA, Franco R, Pintor JJ. Epigenetics in the eye: an overview of the most relevant ocular diseases. *Front Genet*. 2017;8:144.
3. Raeisossadati R, Ferrari MFR, Kihara AH, AlDiri I, Gross JM. Epigenetic regulation of retinal development. *Epigenetics Chromatin*. 2021;14:11.
4. Watanabe S, Murakami A. Regulation of retinal development via the epigenetic modification of histone H3. *Adv Exp Med Biol*. 2016;854:635–641.
5. Shi X, Xue Z, Ye K, et al. Roles of non-coding RNAs in eye development and diseases. *Wiley Interdiscip Rev RNA*. 2023;14:e1785.
6. Lee M, Kim B, Kim VN. Emerging roles of RNA modification: m(6)A and U-tail. *Cell*. 2014;158:980–987.
7. Zhang Y, Lei Y, Dong Y, et al. Emerging roles of RNA ac4C modification and NAT10 in mammalian development and human diseases. *Pharmacol Ther*. 2023;253:108576.
8. Nachtergaele S, He C. The emerging biology of RNA post-transcriptional modifications. *RNA Biol*. 2017;14:156–163.
9. Cayir A. RNA modifications as emerging therapeutic targets. *Wiley Interdiscip Rev RNA*. 2022;13:e1702.
10. Chen Z, Zhao P, Li F, et al. Comprehensive review and assessment of computational methods for predicting RNA post-transcriptional modification sites from RNA sequences. *Brief Bioinform*. 2020;21:1676–1696.
11. Karthiya R, Wasil SM, Khandelia P. Emerging role of N4-acetylcytidine modification of RNA in gene regulation and cellular functions. *Mol Biol Rep*. 2020;47:9189–9199.
12. Jin G, Xu M, Zou M, Duan S. The processing, gene regulation, biological functions, and clinical relevance of N4-acetylcytidine on RNA: a systematic review. *Mol Ther Nucleic Acids*. 2020;20:13–24.
13. Arango D, Sturgill D, Yang R, et al. Direct epitranscriptomic regulation of mammalian translation initiation through N4-acetylcytidine. *Mol Cell*. 2022;82:2912.
14. Luo J, Cao J, Chen C, Xie H. Emerging role of RNA acetylation modification ac4C in diseases: current advances and future challenges. *Biochem Pharmacol*. 2023;213:115628.
15. Hori H. Transfer RNA modification enzymes with a thiouridine synthetase, methyltransferase and pseudouridine synthase (THUMP) domain and the nucleosides they produce in tRNA. *Genes (Basel)*. 2023;14:382.
16. Wei W, Zhang S, Han H, et al. NAT10-mediated ac4C tRNA modification promotes EGFR mRNA translation and gefitinib resistance in cancer. *Cell Rep*. 2023;42:112810.
17. Sharma S, Langhendries JL, Watzinger P, Kötter P, Entian KD, Lafontaine DL. Yeast Kre33 and human NAT10 are conserved 18S rRNA cytosine acetyltransferases that modify tRNAs assisted by the adaptor Tan1/THUMPD1. *Nucleic Acids Res*. 2015;43:2242–2258.
18. Ito S, Horikawa S, Suzuki T, et al. Human NAT10 is an ATP-dependent RNA acetyltransferase responsible for N4-acetylcytidine formation in 18 S ribosomal RNA (rRNA). *J Biol Chem*. 2014;289:35724–35730.
19. Xie L, Zhong X, Cao W, Liu J, Zu X, Chen L. Mechanisms of NAT10 as ac4C writer in diseases. *Mol Ther Nucleic Acids*. 2023;32:359–368.
20. Shang X, Peng Y, Wang Y, et al. Profile analysis of N4-acetylcytidine (ac4C) on mRNA of human lung adenocarcinoma and paired adjacent non-tumor tissues. *Biochim Biophys Acta Gen Subj*. 2023;1867:130498.

Investigative Ophthalmology & Visual Science

21. Liu R, Wubulikasimu Z, Cai R, et al. NAT10-mediated N4-acetylcytidine mRNA modification regulates self-renewal in human embryonic stem cells. *Nucleic Acids Res*. 2023;51:8514–8531.
22. Arango D, Sturgill D, Alhusaini N, et al. Acetylation of cytidine in mRNA promotes translation efficiency. *Cell*. 2018;175:1872–1886.e1824.
23. Tardu M, Jones JD, Kennedy RT, Lin Q, Koutmou KS. Identification and quantification of modified nucleosides in saccharomyces cerevisiae mRNAs. *ACS Chem Biol*. 2019;14:1403–1409.
24. Ito S, Akamatsu Y, Noma A, et al. A single acetylation of 18 S rRNA is essential for biogenesis of the small ribosomal subunit in Saccharomyces cerevisiae. *J Biol Chem* 2014;289:26201–26212.
25. Wang G, Zhang M, Zhang Y, et al. NAT10-mediated mRNA N4-acetylcytidine modification promotes bladder cancer progression. *Clin Transl Med*. 2022;12:e738.
26. Liu X, Cai S, Zhang C, et al. Deacetylation of NAT10 by Sirt1 promotes the transition from rRNA biogenesis to autophagy upon energy stress. *Nucleic Acids Res*. 2018;46:9601–9616.
27. Balmus G, Larrieu D, Barros AC, et al. Targeting of NAT10 enhances healthspan in a mouse model of human accelerated aging syndrome. *Nat Commun*. 2018;9:1700.
28. Broly M, Polevoda BV, Awayda KM, et al. THUMPD1 bi-allelic variants cause loss of tRNA acetylation and a syndromic neurodevelopmental disorder. *Am J Hum Genet*. 2022;109:587–600.
29. Hwang WY, Fu Y, Reyon D, et al. Efficient genome editing in zebrafish using a CRISPR-Cas system. *Nat Biotechnol*. 2013;31:227–229.
30. Ruzicka L, Bradford YM, Frazer K, et al. ZFIN, the zebrafish model organism database: updates and new directions. *Genesis*. 2015;53:498–509.
31. White RJ, Collins JE, Sealy IM, et al. A high-resolution mRNA expression time course of embryonic development in zebrafish. *Elife*. 2017;6:e30860.
32. Liu C, Li R, Li Y, et al. Spatiotemporal mapping of gene expression landscapes and developmental trajectories during zebrafish embryogenesis. *Dev Cell*. 2022;57:1284–1298.e1285.
33. Ciptasari U, van Bokhoven H. The phenomenal epigenome in neurodevelopmental disorders. *Hum Mol Genet*. 2020;29:R42–R50.
34. Reichard J, Zimmer-Bensch G. The epigenome in neurodevelopmental disorders. *Front Neurosci*. 2021;15:776809.
35. Yang Z, Wilkinson E, Cui YH, Li H, He YY. NAT10 regulates the repair of UVB-induced DNA damage and tumorigenicity. *Toxicol Appl Pharmacol*. 2023;477:116688.
36. Dalhat MH, Choudhry H, Khan MI. NAT10, an RNA cytidine acetyltransferase, regulates ferroptosis in cancer cells. *Antioxidants (Basel)*. 2023;12:1116.
37. Zheng X, Wang Q, Zhou Y, et al. N-acetyltransferase 10 promotes colon cancer progression by inhibiting ferroptosis through N4-acetylation and stabilization of ferroptosis suppressor protein 1 (FSP1) mRNA. *Cancer Commun (Lond)*. 2022;42:1347–1366.
38. Zong G, Wang X, Guo X, et al. NAT10-mediated AXL mRNA N4-acetylcytidine modification promotes pancreatic carcinoma progression. *Exp Cell Res*. 2023;428:113620.
39. Chrispell JD, Rebrik TI, Weiss ER. Electroretinogram analysis of the visual response in zebrafish larvae. *J Vis Exp*. 2015;97:e52662.

Investigative Ophthalmology & Visual Science